Published in final edited form as:
Gene Expr Patterns. 2012 August ; 12(7-8): 245–253. doi:10.1016/j.gep.2012.05.002.

Cloning and expression analysis of *Fgf5, 6* and *7* during early chick development

Megha Kumar and **Susan C. Chapman***
Clemson University, Biological Sciences, Long Hall, Clemson, SC 29634, USA

Abstract

FGFs[1] with similar sequences can play different roles depending on the model organisms examined. Determining these roles requires knowledge of spatio-temporal *Fgf* gene expression patterns. In this study, we report the cloning of chick *Fgf5, 6* and *7*, and examine their gene expression patterns by whole mount in situ hybridization. We show that *Fgf5's* spatio-temporally restricted expression pattern indicates a potentially novel role during inner ear development. *Fgf6* and *Fgf7*, although belonging to different subfamilies with diverged sequences, are expressed in similar patterns within the mesoderm. Alignment of protein sequences and phylogenetic analysis demonstrate that FGF5 and FGF6 are highly conserved between chick, human, mouse and zebrafish. FGF7 is similarly conserved except for the zebrafish, which has considerably diverged.

Keywords

Development; Fibroblast growth factor; otic placode; pharyngeal arch; pharyngeal endoderm

1. Introduction

Fibroblast Growth Factor (FGF) signaling is required for cell migration, proliferation and differentiation during embryonic development (Itoh and Ornitz, 2008). FGFs bind to FGF receptors (FGFR) and heparan sulfate oligosaccharides to activate signal transduction in target cells. FGF signaling is regulated by the amount of FGF ligand available and by the regionally restricted expression of FGFs and FGF receptors (FGFR). The specificity of FGFs is further enhanced by the presence of tissue specific modifications in the heparan chains (Ornitz and Marie, 2002). Alternative splicing of the FGFR mRNA results in generation of specific isoforms. The isoforms are tissue specific, as the b-isoform is generated in epithelial cells and c-isoform in mesenchymal cells (Ornitz and Marie, 2002). FGFs serve as mitogens and mediators of cellular differentiation for many ectoderm and mesoderm derived cells, such as fibroblasts, chondrocytes, smooth muscle cells and vascular endothelial cells (Goldfarb, 1990). All FGFs contain a highly conserved 28 amino acid core region (Ornitz, 2000), and 22 FGFs in various vertebrate species, including human, mouse and chick, have been reported. Due to duplication within the zebrafish genome, multiple

*Corresponding author: schapm2@clemson.edu Tel: +1 864 656 5432 Fax: +1 864 656 0435.

Conflict of Interest
The authors declare no conflict of interest.

copies of *Fgf* genes have arisen, often with divergent roles (Itoh, 2007; Itoh and Ornitz, 2008).

FGF signals across epithelial-mesenchymal boundaries play key roles in induction and patterning of adjacent tissues. Craniofacial development requires FGF signaling, with restricted expression in the nasal and midfacial tissues, suggesting that FGFs play a role in patterning these structures (Bachler and Neubuser, 2001). FGFs are also required for otic placode induction, patterning and differentiation of the otic vesicle, cochlea, vestibular system, and the endolymphatic organ (Schimmang, 2007). The pharyngeal arches and subdivisions of the brain show regionalized expression patterns (Lunn et al., 2007). Somitic mesoderm, pharyngeal endoderm and limb bud mesoderm all required FGF signaling (Alvarez et al., 2003; Couly et al., 2002; Schimmang, 2007; Trokovic et al., 2005).

As a first step in understanding the role of FGFs during development it is essential to determine the gene expression patterns of *Fgf* family members in the developing embryo. Although many FGFs can act redundantly, some that show similarity in their spatio-temporal gene expression are not necessarily functionally redundant. A further complication is that the roles of FGFs with similar sequence can differ in their spatio-temporal expression patterns and mechanism of action between species. For example, *Fgf3* and *Fgf8* are expressed in rhombomere 4 (hindbrain) in the zebrafish embryo and both are required for otic induction (Leger and Brand, 2002; Phillips et al., 2001). In mouse, *Fgf3* is expressed in the neuroectoderm, whereas *Fgf10* is expressed in the head mesenchyme, but both are required for otic induction (Wright and Mansour, 2003). In chick, *Fgf19*, expressed in the cephalic paraxial mesoderm, and *Wnt8c* and *Fgf3*, expressed in the hindbrain, are required for otic induction (Ladher et al., 2005). *Fgf15* is the murine homolog of chick *Fgf19. M*ouse FGF15 and chick FGF19 share very low sequence conservation (32.1%) (Wright et al., 2004), yet they share similar expression domains in some tissues such as the primitive streak, pharyngeal pouches and tail bud. However, *Fgf15* is not expressed in the mesoderm underlying the otic placode and, unlike chick FGF19, mouse FGF15 is not required for otic induction (Wright et al., 2004).

In this study, we report the cloning and expression analysis of chick *Fgf5, 6* and *7* during early development. Targeted fragments of *Fgf5, 6* and 7 were used to make riboprobes with the least overlap to FGF family members for in situ hybridization (ISH) analysis during early embryogenesis. Non-consensus probes were used to reduce potential cross-reaction between *Fgf* family members. Our results show regionally restricted spatio-temporal expression patterns. *Fgf5* has a novel expression domain in the nascent otic placode, which bears further investigation. *Fgf6* is expressed in the head mesoderm and pharyngeal arches at early stages. *Fgf7* are expressed in the head mesoderm, but excluded from the pharyngeal arches.

2. Results and Discussion

2.1. Multiple Alignment and Phylogenetic analysis

The amino acid sequences of *Fgf5, 6* and *7* were deduced from NCBI (http://www.ncbi.nlm.nih.gov), and Ensembl (http://www.ensembl.org) database. The four taxa chosen for the phylogenetic study were chick (gg- *Gallus gallus*), mouse (mm- *Mus musculus*), human (hs- *Homo sapiens*) and zebrafish (dr- *Danio rerio*).

Based on multiple alignment analysis, amino acid sequences of FGF5 and FGF6 were highly conserved between all four taxa studied (Fig.1A, B). In zebrafish FGF6a corresponds to the FGF6 sequences in the other taxa. FGF5 and FGF7 are not duplicated in the zebrafish. Although the amino acid sequence of FGF7 indicated high conservation between chick,

mouse and human (Fig. 1C), the zebrafish sequence has diverged, suggesting a diverged role for FGF7 in the fish. Further, the amino acid sequences of all three genes showed a higher percent similarity to their murine counterpart, as compared to the human and zebrafish orthologs (Table 1).

A phylogenetic tree of the amino acid sequence of FGF5, 6 and 7 was generated by the Maximum Likelihood (ML) method in the four taxa (bootstrap replicates, n = 1000) (data not shown). The same tree topology was deduced by the Neighbor Joining (NJ) method (bootstrap replicates, n = 1000). Based on this analysis, FGF5 and FGF6 were more closely related across different vertebrate classes and can be termed as sister groups. FGF7 was an outgroup to both FGF5 and FGF6. For all three proteins, the human and mouse orthologs were more closely related, forming sister clades. The chick orthologs serve as an outgroup for both FGF5 and FGF7. Zebrafish FGF5 and FGF7 were evolutionarily more distant, which corroborated well with our percent similarity and sequence alignment results. Chick and zebrafish FGF6 can be termed sister clades, just as the mouse and human orthologs constitute a sister clade for FGF5 and FGF7.

2.2. Chick FGF5, 6 and 7 bioinformatics analysis

The bioinformatics analyses were performed with Phobius and SignalP 3.0 servers. In addition to Phobius, the Simple Modular Architecture Tool (SMART) from NCBI was used to predict the membrane topology, signal peptides and transmembrane helices (Fig. 1). The Phobius and SMART programs predicted that FGF5 lacks membrane helices and consists of two low complexity segments from amino acid residues 1-14, and the other from amino acid residues 170-183 (Fig. 1A). The SignalP 3.0 results predicted FGF5 to be a non-secretory protein with low probability of having either a signal peptide or signal anchor. On the other hand, the prediction indicated that FGF6 has a signal peptide region (amino acids 1-37), a transmembrane domain (amino acid residues 21-41) and that the remainder of the protein (amino acid residues 38-207) is non-cytoplasmic (Fig. 1B). The signal peptide cleavage site lies between amino acid residues 37 and 38. It was predicted that FGF7 has a cytoplasmic domain (amino acid residues 1-11), short transmembrane domain (amino acid residues 12-31) and a non-cytoplasmic domain (amino acid residues 32-194) (Fig. 1C). The signal peptide region in FGF7 extends from amino acid residues 1-31. The SignalP 3.0 server also predicted a signal anchor for FGF7 and the signal peptide cleavage site between amino acid residues 31and 32.

The Conserved Domain Search Tool (CDART) of NCBI revealed a FGF domain (cd00058), a receptor interaction site and a heparin-binding site (glycine box) for FGF5, 6, and 7 (Fig. 1, hash tags). The PFAM (FGF) domain was predicted to include amino acid residues 23-152 in FGF5, amino acid residues 83-204 in FGF6 and amino acid residues 65-198 in FGF7.

To determine the possible functions of FGF5, 6 and 7, ExPASy proteomics server, Prosite, was used to determine the various protein domains and functional sites. FGF5 was predicted to contain a serine rich region (amino acid residues 1-14), a proline rich region (amino acid residues 153-181), and an HBGF/FGF family domain (amino acid residues 84-107) (Fig. 1A). Serine rich sequences are fairly common amongst signaling proteins, although the functional role of these regions is not well understood. These regions serve multiple functions, such as flexible linkers between protein domains, mRNA splicing, or act as phosphorylation switches during signal transduction (Sim and Creamer, 2002). In addition to their structural role in forming the correct conformation of the mature protein, the proline rich regions are crucial binding sites for different protein-protein interactions (Williamson, 1994). It was predicted that FGF6 contains a HBGF/FGF family domain from amino acid residues 144-167 (Fig. 1B), whereas in FGF7 this domain was predicted to include amino

acid residues 125-148 (Fig. 1C). Further, a prokaryotic membrane lipoprotein attachment site (a post-translational modification) was also predicted for FGF7 at amino acid 32 (not shown).

2.3. Fgf5 gene expression

In mammals FGF5 is a secreted glycoprotein and a member of the FGF4 subfamily (FGF4, 5, 6) and signals via FGF receptors with specific affinities, shown here in decreasing order of affinity - FGFR1c, 2c>3c, 4Δ (Zhang et al., 2006). Our bioinformatics analysis predicts that chick FGF5 has a low probability of a signal peptide or signal anchor in its sequence. Therefore, we postulate that chick FGF5 is secreted via the non-classical secretory mechanism similar to FGF2 (Backhaus et al., 2004). *Fgf5* is expressed in numerous mouse tissues over the course of development, including the endoderm, lateral plate mesoderm, skeletal muscle precursors, limb mesenchyme and cranial acoustic ganglion (Haub and Goldfarb, 1991). It is also expressed in the midbrain, dorsal cerebellum and pons, acoustic and dorsal root ganglia, muscle tissue, and the adult brain (Yaylaoglu et al., 2005). Human FGF5 injected into chick embryo limbs using a viral vector increases proliferation of limb fibroblasts, expansion of the perichondrium and connective tissue at the expense of skeletal muscle development (Clase et al., 2000).

Using an extended range of Hamburger and Hamilton (Hamburger and Hamilton, 1951) stages (HH) 4-19 for the ISH analysis, the earliest we detected specific *Fgf5* expression was at HH8 (Fig. 2A). The most notable feature of expression is that *Fgf5* was specifically expressed in the nascent otic placode around the time of induction. The otic placode is a thickening of ectoderm in the hindbrain region that becomes morphologically apparent at around HH9. Induction requires interactions between multiple FGF proteins and WNT8c in the hindbrain, placode and underlying mesoderm (Ladher et al., 2005). The placode invaginates forming an otic cup, which closes up to form the otic vesicle/otocyst by HH17 (Ohyama et al., 2007). The otic vesicle gives rise to the entire vestibuloacoustic apparatus, including mechanosensory, support, endolymph and vestibulocochlear ganglion cells (Schlosser, 2010).

In our ISH analysis, between HH4 and HH8, low levels of widespread, non-specific *Fgf5* expression were detected within embryonic tissues of the area pellucida (not shown). At HH8, a more specific pattern emerged, with expression in the nascent otic placode region (Fig. 2A, arrowhead). In section, the neural tube, otic placode and underlying pharyngeal endoderm were specifically labeled at this anterior-posterior level (Fig. 2B). By HH9, expression was regionalized to the midbrain and the hindbrain region corresponding to rhombomeres 2-6 (Fig. 2C). Sections revealed strong expression in the neural tube, pharyngeal endoderm and otic placode as invagination begins (Fig. 2D, E). By HH11, the expression was restricted to the dorsal neural tube at the level of the midbrain and the invaginating otic cup (Fig. 2F-H). By HH13, *Fgf5* expression was becoming more widespread, expanding into the head mesoderm in the rostral embryo (Fig. 2I). This upregulation of expression was evident in section, at the level of the otic cup (fig. 2J). From HH15, expression was upregulated within the trunk mesoderm in an anterior to posterior wave, becoming widely expressed throughout the embryonic mesoderm (Fig. 2K). At HH18, the first hint of expression in the hindlimb bud mesenchyme was noted (Fig. 2L, asterisk). Sections showed expression was restricted to the mesoderm and excluded from the neural tube, notochord, and eye tissue (Fig. 2M). At the level of the 2nd arch the otic vesicle had a spot of expression in the medial domain (Fig. 2N, arrowed). The widespread mesoderm expression in chick was similar to that of the mouse at these early stages (Haub and Goldfarb, 1991). Additionally, the chick *Fgf5* expression pattern suggests a potentially novel role in induction or regionalization of the otic placode.

2.4. Fgf6 gene expression

FGF6, another member of the FGF4 subfamily, has reported roles in mouse myogenesis and is expressed in the somitic myotome and later in the skeletal muscle tissues (Armand et al., 2006a). *Fgf6* is also expressed in the mouth, tongue, pharyngeal and neck muscles. Additionally, FGF6 is a regulator of bone metabolism (Armand et al., 2006b; deLapeyriere et al., 1993; Han and Martin, 1993; Rescan, 1998). As a member of the FGF4 subfamily, receptor affinity is the same as for FGF5 (Zhang et al., 2006).

In situ hybridization analysis was conducted on whole mount chick embryos from HH8-19. The earliest chick *Fgf6* expression was detected in our in situ hybridization analysis was HH14 (Fig. 3A). Expression was detected in the pharyngeal and visceral endoderm, with transcripts also in the adjacent trunk and head mesoderm (Fig. 3A-E). At all stages examined the neural tube, notochord, surface ectoderm, otic vesicle (Fig. 3E, J, O) and eyes (Fig. 3G, L) were negative for expression. At HH17, expression was upregulated in the head, pharyngeal arch and foregut mesoderm, with weak expression detected in the posterior embryo (Fig. 3F-H). By HH19, strong hindgut and visceral mesoderm expression was detected in the posterior embryo (Fig. 3K-M). Thus, during early development *Fgf6* is widely expressed in head, pharyngeal and visceral mesoderm. Our expression analysis is broadly in line with that reported in the mouse (deLapeyriere et al., 1993).

2.5. Fgf7 gene expression

FGF7, together with FGF10 and FGF22 composes the FGF7 subfamily. FGF7 is mainly transduced through FGFR2b, and less so through FGFR1b (Zhang et al., 2006). FGF7, also known as Keratinocyte Growth Factor (KGF), is an epithelial mitogen that acts as a diffusible mediator. FGF7 is mainly expressed in mesoderm tissues and acts via FGF receptors in epithelial tissue in a classical epithelial mesenchymal interaction (Finch and Rubin, 2004a; Mason et al., 1994; Post et al., 1996). For example, mouse *Fgf7* is expressed during lung development in the mesenchyme and FGFR2b, its receptor, is located in the adjacent airway epithelium (Post et al., 1996). *Fgf7* is expressed in multiple tissues during mouse development (Finch et al., 1995; Mason et al., 1994), including the mesenchyme surrounding the mouse mammary bud (Mailleux et al., 2002), and has roles in branching morphogenesis of hepatic and submandibular glands (Hoffman et al., 2002; Steinberg et al., 2005).

Functional studies using recombinant human protein show proliferation, migration and differentiation roles for FGF7, especially following skin and mucosal tissue injury (Finch and Rubin, 2004b). FGF7 also induces an AER in competent tissue (Yonei-Tamura et al., 1999). Application of FGF7 recombinant protein mimics the action of all FGFR2 binding proteins. However, it must be noted that these studies are not necessarily an indication of the endogenous role of FGF7. The mouse FGF10 knockout, which shows failure of lung development (Sekine et al., 1999), supports this hypothesis. Loss of FGF10 is catastrophic for organs requiring branching morphogenesis, such as the lungs, liver and pancreas. FGF7 does not act redundantly to rescue development, but can do so when added exogenously (Finch and Rubin, 2004a). Nonetheless, these functional experiments demonstrate the therapeutic potential of FGF7.

In chick, the only expression previously reported put *Fgf7* expression in the mesenchyme and smooth muscle of the gizzard at later stages, E6-E7 (Shin et al., 2003; Shin et al., 2005). In our study at early developmental stages, *Fgf7* expression was first detected in the mesoderm and pharyngeal endoderm at HH14 (Fig. 4A). We analyzed younger embryos, from HH8-13, but no transcripts were detected. At HH16, expression expanded into the head mesoderm and was restricted to pharyngeal endoderm (Fig. C-E). By HH18, expression was

more widespread in the head mesoderm and pharyngeal endoderm (Fig. 4F-H). At HH19, expression was detected in more mesoderm tissue, with the exception of the pharyngeal arches which remained negative for transcripts (Fig. 4I, J). Neural tube, eye and notochord (Fig. 4E, H, K) were negative for expression in all stages tested, as was the otic vesicle (Fig. 4B, D, G, J). In the posterior embryo, the hindgut and adjacent mesoderm, the trunk mesoderm and medial mesoderm of the hind limb buds all had expression (Fig. 4L). Although superficially similar to *Fgf6* expression, our analysis reveals that there are subtle differences in spatiotemporal expression patterns between Fgf6 and Fgf7.

2.6. Conclusion

We have described the expression patterns of *Fgf5, 6* and *7* during early embryogenesis and performed bioinformatics analysis. The regionally restricted expression of *Fgf5* in the inner ear is novel and requires further examination. *Fgf6* and *Fgf7* share similar expression patterns, however, their roles are separated in mice and humans, with *Fgf6* involved in myogenesis (Armand et al., 2006a) and *Fgf7* having an important role as an epithelial mitogen (Finch and Rubin, 2004a; Mason et al., 1994; Post et al., 1996). Since there are numerous *Fgf* genes with overlapping expression the availability of appropriate receptors seems to be a critical factor (Trokovic et al., 2005). Although the receptor affinities for FGF molecules have been reported for the mouse, they have not been reported in the chick and it is, therefore, not clear if the affinities are comparable. A recent detailed chick FGF receptor expression study provides some insight into potentially important regions of ligand-receptor interaction (Nishita et al., 2011). For example, FGF5 and FGF6 act mainly through FGFR1c and 2c, whereas FGF7 acts through FGFR2b. At stage 9, FGFR1c and 2c are expressed in the neural tube, with *Fgf5* expression in the neural tube, otic placode and adjacent pharyngeal endoderm, suggesting that active signaling may be taking place in the region of the otic placode. No *Fgf6* or *Fgf7* expression is detected until HH14. At stage 13, however, FGFR1c and 2c are detected along the length of the neural tube with differential expression in the diencephalon and optic cups. FGFR2b, the main receptor for FGF7 is restricted to the thyroid rudiment. Taken together these data support a model in which the receptors and specific receptor affinities act to ensure tissue specific signaling between multiple, overlapping *Fgf* gene expression patterns.

3. Experimental procedures

3.1 Isolation and cloning of Fgf5, 6 and 7

In order to clone the chick orthologs of *Fgf5, 6* and *7*, we used sequence specific nested primers for each of the genes designed according to the chick reference sequences (www.ensemble.org) (Table 2). Nested primers for each gene were used to ensure that other FGF family members were not simultaneously amplified. Expected sequences were checked against full-length *Fgf* family members to ensure they had the minimum overlap and would not recognize family members during ISH analysis. *Fgf5* cDNA was obtained from the total RNA isolated from the limbs of E7 Bovan Brown x Rhode Island Red chick embryos (Morgan Poultry Center, Clemson University) by reverse transcription PCR (RT-PCR). *Fgf6* and *Fgf7* cDNA was obtained from total RNA isolated from the trunk region of the HH21 embryos. Reverse transcription was carried out for 45 min at 45°C using a reverse transcription kit (Promega, A1260), followed by PCR amplification using 1 cycle of 94°C for 2 min, 30 cycles of 94°C, 59°C and 68°C for 1 min each, and a final extension cycle of 68°C for 7 min. The amplified product was cloned into the PCRII TOPO vector (Invitrogen) and sequenced at the Clemson University Genomics Institute. Clone fragments were obtained for *Fgf5* (base pairs 162-500, ENSGALG00000010893) *Fgf6* (base pairs 106-402, ENSGALG00000017287) and *Fgf7* (base pairs 377-601, ENSGALG00000005671). Probes using the entire fragment were made as follows: a linearized fragment of *Fgf5* was made by

PCR using M13 Forward and Reverse primers and transcribed with T7. *Fgf6* and *Fgf7* were linearized with HindIII and transcribed with T7.

3.2. Embryos and in situ hybridization analysis

Fertile chicken eggs from Bovan Brown x Rhode Island Red mating were incubated to the desired stages at 38.5 °C in a humidified forced air incubator. Staging was done according to the normal table of Hamburger and Hamilton (Hamburger and Hamilton, 1951). ISH was performed as previously described (Chapman et al., 2002). No signal was observed using the control sense probes.

3.3. Image analysis

After color visualization and fixation in 4% paraformaldehyde (PFA) the processed embryos were cleared in 80% glycerol/phosphate buffered saline (PBS) and photographed in whole mount. Embryos were rinsed several times in PBS and embedded in 20% gelatin/PBS and fixed in 4% PFA/PBS for a minimum of three days before sectioning. Embryos were sectioned at 50 μm using a Leica vibratome, mounted in 80% glycerol/PBS and coverslipped. Images were obtained using a Nikon SMZ1500 stereomicroscope or Q-Imaging 5MPV camera. Images were edited with Adobe Photoshop CS4.

3.4. Methods of sequence analysis

The amino acid sequences of FGF5, 6 and 7 for the four taxa were obtained from the NCBI or Ensembl database as follows: FGF5 - chick (Ensembl ID: ENSGALP00000017695), mouse (GenBank ID: AAH71227), human (GenBank ID: AAB06463), zebrafish (GenBank ID: BAD69616); FGF6 - chick (ENSGALP00000027889), mouse (GenBank ID: AAA62261), human (GenBank ID: EAW88847), zebrafish (FGF6a) (GenBank ID: AAO15997); FGF7 - chick (GenBank ID : NP_001012543), mouse (GenBank ID: AAH52847), human (GenBank ID: AAA63210) and zebrafish (GenBank ID: BAD69716.1).

Multiple sequence alignments were performed using the MUSCLE algorithm in the SeaView 4.1.12 program (http://pbil.univ-lyon1.fr/software/seaview.html) (Gouy et al., 2010). The 60% threshold value was used to generate the consensus sequence among the four taxa for all the three genes with no gaps allowed. The LALIGN program (http://www.ebi.ac.uk/Tools/psa/lalign) was used to determine the percent identity between nucleotide and protein sequences of chick *Fgf5, 6* and *7* with the mouse, human and zebrafish orthologs. The LALIGN program used the Smith-Waterman algorithm with Blosum50 as the scoring matrix for the protein sequences (Huang and Miller, 1991).

Phylogenetic analysis was performed using the Maximum Likelihood (ML) and Neighborhood Joining (NJ) approaches using the SeaView 4.1.12 program. For the ML approach, the tree was constructed using the PhyML program with the LG model of amino acid substitution. The presence of invariable sites and site rate variation were optimized, and the most likely tree was searched using best of Nearest-Neighbor Interchange (NNI) and Subtree Pruning and Regrafting (SPR) option. For the NJ method, the distance tree was constructed using the Poisson distance and the BioNJ tree-building algorithm. The confidence of each node was assessed by 1000 bootstrap replicates for each approach. The Prosite (http://expasy.org/prosite and http://expasy.org/tools/scanprosite) database was used to determine the different protein domains, families and functional sites. The Prosite search used the UniProt, SwissProt and PDB databases. Patterns with a high probability of occurrence were included and no filters were used to identify the different domains. Conserved Domains Search Tool (CDART, http://www.ncbi.nlm.nih.gov/Structure/cdd/wrpsb.cgi) and Simple Modular Architecture Tool (SMART, http://smart.embl-heidelberg.de) were used to identify PFAM domains,

internal repeats and conserved FGF domains. The potential signal peptides were predicted using the Phobius (http://phobius.sbc.su.se) and SignalP 3.0 server (http://www.cbs.dtu.dk/services/SignalP-3.0) and using the Neural Network (NN) and Hidden Markov Model (HMM) prediction.

Acknowledgments

This study was supported by an NIH/NIDCD grant DC009236 and ARRA supplemental funding. Technical Contribution No. 5993 of the Clemson University Experiment Station. We thank Ms. Kristin Beard, Department of Genetics and Biochemistry, Clemson University for technical assistance in the phylogenetic analysis.

Abbreviations

FGF/*Fgf*	Fibroblast Growth Factor
FGFR	FGF receptor
ISH	*in situ* hybridization

References

Alvarez Y, Alonso MT, Vendrell V, Zelarayan LC, Chamero P, Theil T, Bosl MR, Kato S, Maconochie M, Riethmacher D, Schimmang T. Requirements for FGF3 and FGF10 during inner ear formation. Development. 2003; 130:6329–6338. [PubMed: 14623822]

Armand AS, Laziz I, Chanoine C. FGF6 in myogenesis. Biochimica et biophysica acta. 2006a; 1763:773–778. [PubMed: 16875743]

Armand AS, Laziz I, Chanoine C. FGF6 in myogenesis. Biochim Biophys Acta. 2006b; 1763:773–778. [PubMed: 16875743]

Bachler M, Neubuser A. Expression of members of the Fgf family and their receptors during midfacial development. Mechanisms of development. 2001; 100:313–316. [PubMed: 11165488]

Backhaus R, Zehe C, Wegehingel S, Kehlenbach A, Schwappach B, Nickel W. Unconventional protein secretion: membrane translocation of FGF-2 does not require protein unfolding. J Cell Sci. 2004; 117:1727–1736. [PubMed: 15075234]

Chapman SC, Schubert FR, Schoenwolf GC, Lumsden A. Analysis of spatial and temporal gene expression patterns in blastula and gastrula stage chick embryos. Dev Biol. 2002; 245:187–199. [PubMed: 11969265]

Clase KL, Mitchell PJ, Ward PJ, Dorman CM, Johnson SE, Hannon K. FGF5 stimulates expansion of connective tissue fibroblasts and inhibits skeletal muscle development in the limb. Dev Dyn. 2000; 219:368–380. [PubMed: 11066093]

Couly G, Creuzet S, Bennaceur S, Vincent C, Le Douarin NM. Interactions between Hox-negative cephalic neural crest cells and the foregut endoderm in patterning the facial skeleton in the vertebrate head. Development. 2002; 129:1061–1073. [PubMed: 11861488]

deLapeyriere O, Ollendorff V, Planche J, Ott MO, Pizette S, Coulier F, Birnbaum D. Expression of the Fgf6 gene is restricted to developing skeletal muscle in the mouse embryo. Development. 1993; 118:601–611. [PubMed: 8223280]

Finch PW, Cunha GR, Rubin JS, Wong J, Ron D. Pattern of keratinocyte growth factor and keratinocyte growth factor receptor expression during mouse fetal development suggests a role in mediating morphogenetic mesenchymal-epithelial interactions. Developmental dynamics : an official publication of the American Association of Anatomists. 1995; 203:223–240. [PubMed: 7655084]

Finch PW, Rubin JS. Keratinocyte growth factor/fibroblast growth factor 7, a homeostatic factor with therapeutic potential for epithelial protection and repair. Adv Cancer Res. 2004a; 91:69–136. [PubMed: 15327889]

Finch PW, Rubin JS. Keratinocyte growth factor/fibroblast growth factor 7, a homeostatic factor with therapeutic potential for epithelial protection and repair. Advances in cancer research. 2004b; 91:69–136. [PubMed: 15327889]

Goldfarb M. The fibroblast growth factor family. Cell growth & differentiation : the molecular biology journal of the American Association for Cancer Research. 1990; 1:439–445.

Gouy M, Guindon S, Gascuel O. SeaView version 4: A multiplatform graphical user interface for sequence alignment and phylogenetic tree building. Mol Biol Evol. 2010; 27:221–224. [PubMed: 19854763]

Hamburger V, Hamilton HL. A series of normal stages in the development of the chick embryo. J Morphol. 1951; 88:49–92.

Han JK, Martin GR. Embryonic expression of Fgf-6 is restricted to the skeletal muscle lineage. Dev Biol. 1993; 158:549–554. [PubMed: 8344469]

Haub O, Goldfarb M. Expression of the fibroblast growth factor-5 gene in the mouse embryo. Development. 1991; 112:397–406. [PubMed: 1794310]

Hoffman MP, Kidder BL, Steinberg ZL, Lakhani S, Ho S, Kleinman HK, Larsen M. Gene expression profiles of mouse submandibular gland development: FGFR1 regulates branching morphogenesis in vitro through BMP- and FGF-dependent mechanisms. Development. 2002; 129:5767–5778. [PubMed: 12421715]

Huang X, Miller W. A time-efficient, linear-space local similarity algorithm. Adv. Appl. Math. 1991; 12:337–357.

Itoh N. The Fgf families in humans, mice, and zebrafish: their evolutional processes and roles in development, metabolism, and disease. Biol Pharm Bull. 2007; 30:1819–1825. [PubMed: 17917244]

Itoh N, Ornitz DM. Functional evolutionary history of the mouse Fgf gene family. Developmental dynamics : an official publication of the American Association of Anatomists. 2008; 237:18–27. [PubMed: 18058912]

Ladher RK, Wright TJ, Moon AM, Mansour SL, Schoenwolf GC. FGF8 initiates inner ear induction in chick and mouse. Genes Dev. 2005; 19:603–613. [PubMed: 15741321]

Leger S, Brand M. Fgf8 and Fgf3 are required for zebrafish ear placode induction, maintenance and inner ear patterning. Mechanisms of development. 2002; 119:91–108. [PubMed: 12385757]

Lunn JS, Fishwick KJ, Halley PA, Storey KG. A spatial and temporal map of FGF/Erk1/2 activity and response repertoires in the early chick embryo. Developmental biology. 2007; 302:536–552. [PubMed: 17123506]

Mailleux AA, Spencer-Dene B, Dillon C, Ndiaye D, Savona-Baron C, Itoh N, Kato S, Dickson C, Thiery JP, Bellusci S. Role of FGF10/FGFR2b signaling during mammary gland development in the mouse embryo. Development. 2002; 129:53–60. [PubMed: 11782400]

Mason IJ, Fuller-Pace F, Smith R, Dickson C. FGF-7 (keratinocyte growth factor) expression during mouse development suggests roles in myogenesis, forebrain regionalisation and epithelial-mesenchymal interactions. Mech Dev. 1994; 45:15–30. [PubMed: 8186145]

Nishita J, Ohta S, Bleyl SB, Schoenwolf GC. Detection of isoform-specific fibroblast growth factor receptors by whole-mount in situ hybridization in early chick embryos. Developmental dynamics : an official publication of the American Association of Anatomists. 2011; 240:1537–1547. [PubMed: 21465617]

Ohyama T, Groves AK, Martin K. The first steps towards hearing: mechanisms of otic placode induction. The International journal of developmental biology. 2007; 51:463–472. [PubMed: 17891709]

Ornitz DM. FGFs, heparan sulfate and FGFRs: complex interactions essential for development. Bioessays. 2000; 22:108–112. [PubMed: 10655030]

Ornitz DM, Marie PJ. FGF signaling pathways in endochondral and intramembranous bone development and human genetic disease. Genes & development. 2002; 16:1446–1465. [PubMed: 12080084]

Phillips BT, Bolding K, Riley BB. Zebrafish fgf3 and fgf8 encode redundant functions required for otic placode induction. Developmental biology. 2001; 235:351–365. [PubMed: 11437442]

Post M, Souza P, Liu J, Tseu I, Wang J, Kuliszewski M, Tanswell AK. Keratinocyte growth factor and its receptor are involved in regulating early lung branching. Development. 1996; 122:3107–3115. [PubMed: 8898224]

Rescan PY. Identification of a fibroblast growth factor 6 (FGF6) gene in a non-mammalian vertebrate: continuous expression of FGF6 accompanies muscle fiber hyperplasia. Biochimica et biophysica acta. 1998; 1443:305–314. [PubMed: 9878802]

Schimmang T. Expression and functions of FGF ligands during early otic development. The International journal of developmental biology. 2007; 51:473–481. [PubMed: 17891710]

Schlosser G. Making senses development of vertebrate cranial placodes. Int Rev Cell Mol Biol. 2010; 283:129–234. [PubMed: 20801420]

Sekine K, Ohuchi H, Fujiwara M, Yamasaki M, Yoshizawa T, Sato T, Yagishita N, Matsui D, Koga Y, Itoh N, Kato S. Fgf10 is essential for limb and lung formation. Nat Genet. 1999; 21:138–141. [PubMed: 9916808]

Shin M, Fukuda K, Yasugi S. Expression of DDSG1, a novel gene encoding a putative DNA-binding protein in the embryonic chicken nervous system. Gene expression patterns : GEP. 2003; 3:431–436. [PubMed: 12915307]

Shin M, Watanuki K, Yasugi S. Expression of Fgf10 and Fgf receptors during development of the embryonic chicken stomach. Gene expression patterns : GEP. 2005; 5:511–516. [PubMed: 15749079]

Sim KL, Creamer TP. Abundance and distributions of eukaryote protein simple sequences. Mol Cell Proteomics. 2002; 1:983–995. [PubMed: 12543934]

Steinberg Z, Myers C, Heim VM, Lathrop CA, Rebustini IT, Stewart JS, Larsen M, Hoffman MP. FGFR2b signaling regulates ex vivo submandibular gland epithelial cell proliferation and branching morphogenesis. Development. 2005; 132:1223–1234. [PubMed: 15716343]

Trokovic N, Trokovic R, Partanen J. Fibroblast growth factor signalling and regional specification of the pharyngeal ectoderm. The International journal of developmental biology. 2005; 49:797–805. [PubMed: 16172976]

Williamson MP. The structure and function of proline-rich regions in proteins. Biochem J. 1994; 297(Pt 2):249–260. [PubMed: 8297327]

Wright TJ, Ladher R, McWhirter J, Murre C, Schoenwolf GC, Mansour SL. Mouse FGF15 is the ortholog of human and chick FGF19, but is not uniquely required for otic induction. Developmental biology. 2004; 269:264–275. [PubMed: 15081372]

Wright TJ, Mansour SL. Fgf3 and Fgf10 are required for mouse otic placode induction. Development. 2003; 130:3379–3390. [PubMed: 12810586]

Yaylaoglu MB, Titmus A, Visel A, Alvarez-Bolado G, Thaller C, Eichele G. Comprehensive expression atlas of fibroblast growth factors and their receptors generated by a novel robotic in situ hybridization platform. Dev Dyn. 2005; 234:371–386. [PubMed: 16123981]

Yonei-Tamura S, Endo T, Yajima H, Ohuchi H, Ide H, Tamura K. FGF7 and FGF10 directly induce the apical ectodermal ridge in chick embryos. Developmental biology. 1999; 211:133–143. [PubMed: 10373311]

Zhang X, Ibrahimi OA, Olsen SK, Umemori H, Mohammadi M, Ornitz DM. Receptor specificity of the fibroblast growth factor family. The complete mammalian FGF family. J Biol Chem. 2006; 281:15694–15700. [PubMed: 16597617]

Highlights

- Cloning and gene expression analysis of *Fgf5, 6* and *7* in chick
- *Fgf5* is expressed in the otic placode at early stages of development
- *Fgf6* and *7* are broadly expressed in mesoderm tissues
- FGF5, 6 and 7 are highly conserved between chick, human and mouse

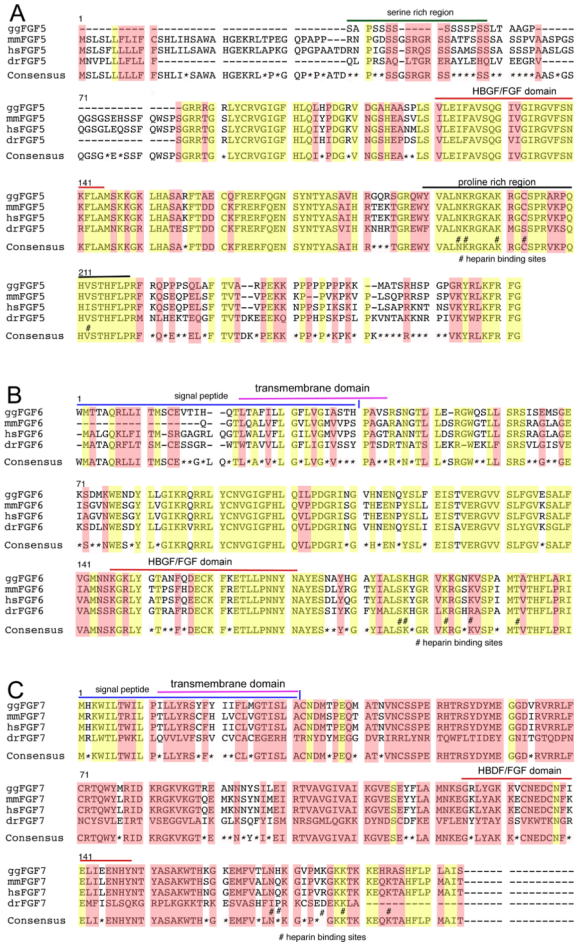

Figure 1. Multiple sequence alignments

Amino acid sequence alignment of chick FGF5 (**A**), FGF6 (**B**) and FGF7 (**C**) with their vertebrate orthologs using the MUSCLE algorithm. Amino acid sequences of chick (gg-*Gallus gallus*), mouse (mm- *Mus musculus*), human (hs- *Homo sapiens*) and zebrafish (dr-*Danio rerio*) are shown. The sequences were obtained from Ensembl (http://www.ensembl.org) and NCBI database (http://www.ncbi.nlm.nih.gov). The conserved amino acids (with 60% threshold) are shown below the alignment. Sequences with 100% similarity are shown in yellow followed by the highly similar sequences shown in pink. Unmarked regions indicate low or no similarity. The horizontal blue line indicates the signal peptide sequence and the vertical blue line indicates the signal peptide cleavage sites and the pink line that transmembrane domain in each alignment. Red lines indicated the conserved HBGF/FGF domains. In FGF5, the green horizontal line indicates the serine rich region and the black line indicates the proline rich region. Hash marks indicate heparin-binding sites. All sites are marked with respect to the gallus sequence.

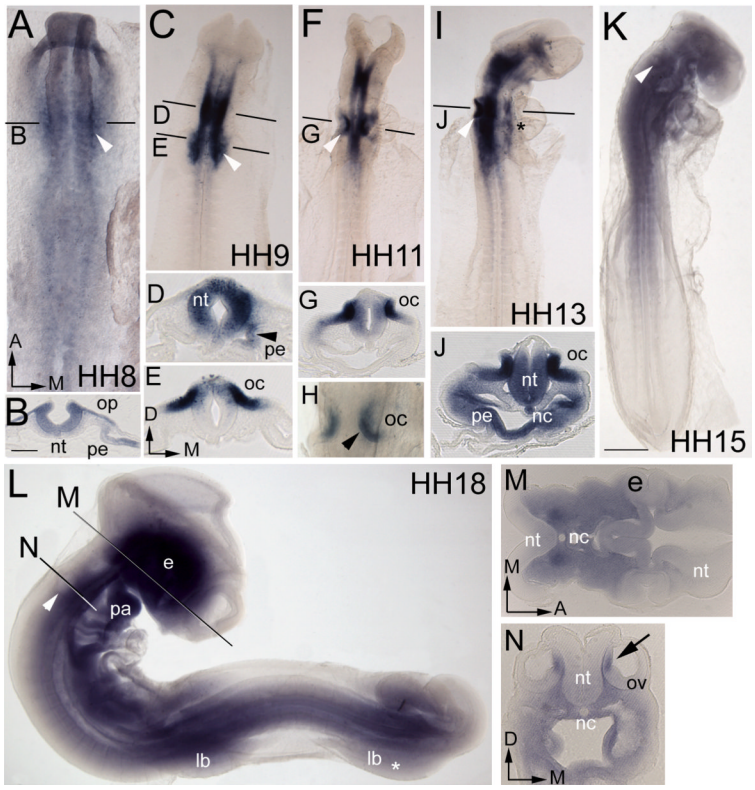

Figure 2. Expression analysis of chick *Fgf5* during early development

Fgf5 expression from stages HH8-18. **(A-N)**. Transverse gelatin sections, 50 μm. White arrowheads indicate otic tissues. (**A, B**) HH8 embryos had widespread *Fgf5* expression in the neuroectoderm, with more specific expression in the region of the nascent otic placode (white arrowhead). (**B**) Neural tube, otic placode and pharyngeal endoderm expression was detected in sections. (**C, D**) HH9 had specific midbrain and hindbrain Fgf5 expression. (**E**) At this level the otic placode and dorsal neural tube were labeled. (**F, G**) At HH11, the invaginating otic cup continued to express Fgf5. (**H**) A dorsal view of the hindbrain region showing otic expression. (**I, J**) *Fgf5* expression expanded at HH13, with neural tube, notochord, mesenchyme, pharyngeal endoderm and distal pharyngeal arches (asterisk) all exhibiting upregulated expression levels. (**K**) At HH15, *Fgf5* expression was becoming widespread within the mesoderm and appearing more posteriorly. (**L**) By HH18, mesoderm expression extended from anterior to posterior. (**M**) In section, at the level of the eyes, the mesoderm is labeled, but neuroectoderm, eyes and notochord are negative for expression. (**N**) At the level of the 2nd arch the only otic expression was in a medial spot (arrowed). Abbreviations; e, eye; nc, notochord; nt, neural tube; lb, limb bud; oc, otic cup; op, otic placode; ov, otic vesicle; pa, pharyngeal arches; pe, pharyngeal endoderm. Scale bars: K, whole mount embryos 200 μm; B, sections 100 μm.

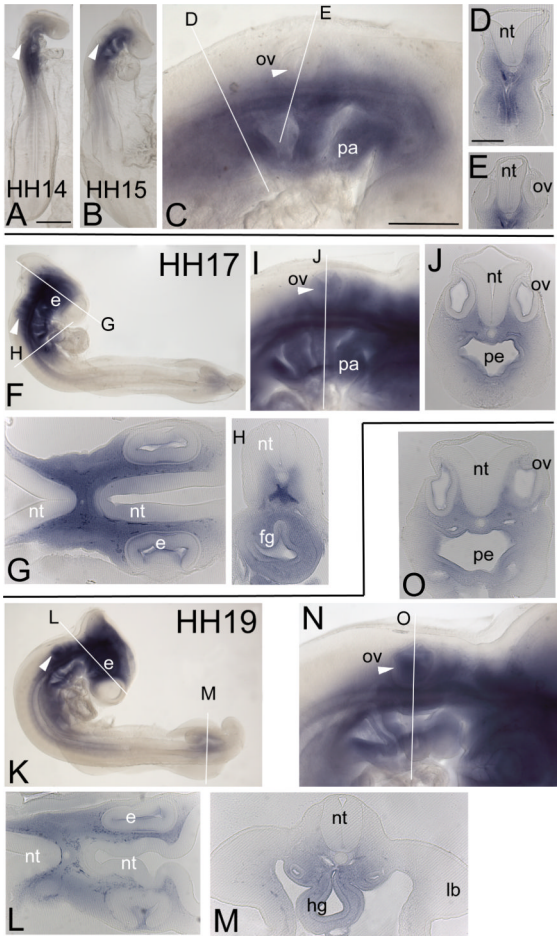

Figure 3. Expression of chick *Fgf6* during early development

Fgf6 expression between HH14-19. Gelatin sections, 50 μm. The otic vesicle is indicated by a white arrowhead in all cases. White lines on whole mounts indicate level and orientation of section. (**A**) *Fgf6* expression is first detected at HH14 in the hindbrain mesoderm. (**B**) Expression is induced rostrally to the level of Rathke's pouch and is observed in the visceral mesoderm and pharyngeal arch mesoderm. (**C**) A magnified view of the hindbrain at HH15. (**D, E**) Sections at the level of the foregut and 2nd arch show foregut endoderm and mesoderm labeling. The otic vesicle is negative. (**F**) At HH17, expression continues to upregulate in the head mesoderm and weak expression in the posterior embryo is detected. (**G, H**) The eye, neural tube and notochord are negative for expression. The head mesoderm, foregut and surrounding mesoderm are labeled. (**I**) In the magnified region of the hindbrain there is extensive mesoderm labeling. (**J**) In section, the head mesoderm and pharyngeal endoderm are labeled, with the neural tube, otic vesicle, notochord and surface ectoderm negative for expression. (**K-O**) At HH19, expression is maintained, with hindgut expression in the posterior embryo. The limb buds are negative for expression. Abbreviations: e, eye; fg, foregut; hg, hindgut; n, notochord; nt, neural tube; ov, otic vesicle; pa, pharyngeal arch; pe, pharyngeal endoderm. Scale bars: A, whole mounts 200 μm; D, sections 100 μm; C, magnified images 500 μm.

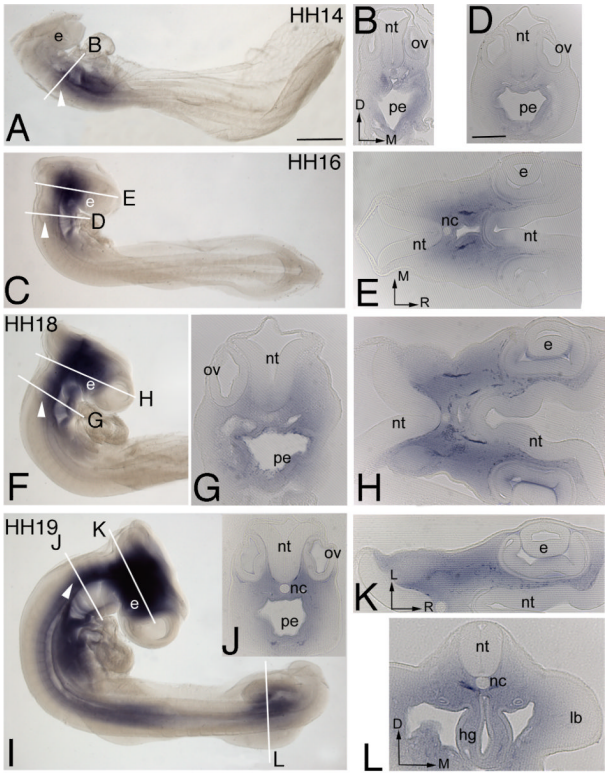

Figure 4. ***Fgf7*** **expression during early stages of chick development**

Fgf7 expression between HH14-19. Gelatin sections, 50 μm. The otic vesicle is indicated by a white arrowhead in whole mount embryos. White lines indicate level of section and orientation. (**A, B**) No expression is detected before HH14, when expression in visceral endoderm and surrounding mesoderm. (**C-E**) At HH16, expression extends rostrally into head mesoderm and is only weakly expressed in pharyngeal endoderm. (**F-H**) At HH18, expression expands into surrounding mesoderm, but is excluded from the neural tube, eye, otic vesicle and surface ectoderm. The pharyngeal arches are all negative for expression. (I) At HH19, mesoderm expression expand toward the posterior. (J, K) Expression continues as for HH18. (L) In the posterior embryo the trunk, hindgut and limb bud mesoderm all have Fgf7 expression. The neural tube, notochord and surface ectoderm are all negative for expression. Abbreviations: e, eye; hg, hindgut; n, notochord; nt, neural tube; ov, otic vesicle; pa, pharyngeal arch; pe, pharyngeal endoderm. Scale bars: A, whole mounts 200 μm; D, sections 100 μm.

Table 1

Percentage identity between DNA and protein sequences of chick compared to mouse, human and zebrafish sequences.

	Mouse	Human	Zebrafish
Chick *Fgf 5*	69.7%	66.5%	61.1%
Chick FGF5	70.0%	66.8%	62.0%
Chick *Fgf 6*	64.8%	64.9%	69.7%
Chick FGF6	70.2%	66.8%	69.4%
Chick *Fgf 7*	81.6%	84.7%	60.7%
Chick FGF7	83.0%	79.9%	58.5%

Table 2

Nested primer sets for cloning of *Fgf5, 6* and *7*.

		Forward primer (5′-3′)	**Reverse primer (5′-3′)**
Fgf 5	Outer set Inner set	TCCGCGCCTTCATCCTCC CAGCGTCCTGGAAATCTTTGCTGT	CTACCCAAAGCGAAACTTTAGCCG ACAGTGAAAGCCAACTGGGATGGT
Fgf 6	Outer set Inner set	TCAACACACCCAGCTGTAAGCAGA ACACACCCAGCTGTAAGCAGAAGT	ACGAAGAGAGCACTTTCCACACCA GCACTTTCCACACCAAACAGGCTT
Fgf 7	Outer set Inner set	TCATGAACACCCAGAACACTGCAC AACAGTGGCAGTTGGAAIAGTGGC	ACCCTTCATGGGAACACCTTTGTG CCTTCATGGGAACACCTTTGTGGT